Journal of Chromatography A, 1220 (2012) 21–25

Contents lists available at SciVerse ScienceDirect

Journal of Chromatography A

journal homepage: www.elsevier.com/locate/chroma

Modelling and optimisation of preparative chromatographic purification of europium

Frida Ojala[a], Mark Max-Hansen[a], Dejene Kifle[b], Niklas Borg[a], Bernt Nilsson[a,*]

[a] Department of Chemical Engineering, Centre for Chemistry and Chemical Engineering, Lund University, P.O. Box 124, SE-221 00 Lund, Sweden
[b] Department of Chemistry, University of Oslo, P.O. Box 1033 Blindern, N-0315 Oslo, Norway

ARTICLE INFO

Article history:
Received 18 July 2011
Received in revised form 7 November 2011
Accepted 17 November 2011
Available online 23 November 2011

Keywords:
Ion-exchange chromatography
Rare earth elements
Europium
Calibration
Optimisation
Kinetic dispersive model

ABSTRACT

A model commonly used to describe the separation of biomolecules was used to simulate the harsh environment when eluting neodymium, samarium, europium and gadolinium with a hot acid. After calibration, the model was used to optimise the preparative separation of europium, as this is the most valuable of the four elements. A kinetic dispersive model with a Langmuir mobile phase modulator isotherm was used to describe the process. The equilibration constant, the stoichiometric coefficient and the column capacity for the components were calibrated. The model fitted the experimental observations well. Optimisation was achieved using a differential evolution method. As the two objective functions used in optimising the process, productivity and yield, are competing objectives, the result was not a single set point but a Pareto front.

1. Introduction

Rare-earth elements are currently used in many electronic devices due to their specific properties, and the demand for these elements in pure fractions is increasing. The source of rare-earth elements is minerals consisting of mixtures of several rare earths, and it is thus necessary to separate them. The price of rare-earth elements increases with the demand on purity [1], and it is therefore of economic interest to purify the elements to a high level, provided a cost-effective separation process is available. However, it is not easy to separate these elements as they have similar chemical properties [2]. Commercial separation is usually carried out using liquid–liquid extraction, while small-scale separation is often performed by means of preparative ion-exchange chromatography [2]. Small-scale separation is utilised when the demands on purity are high, and the elements of interest are of high value.

The subject of this study was the separation of the elements neodymium (Nd), samarium (Sm), europium (Eu) and gadolinium (Gd) by preparative ion-exchange chromatography. Europium is the most valuable of the four elements [1], and this was the target component for purification. Cerium was used in the overloaded experiments, as it was believed to have similar properties to the other elements but is cheaper; making it more suitable when large quantities are required. To minimise the cost of purifying the elements while ensuring the desired level of purity, it is essential to optimise the separation process. Computer simulation was used to shorten the optimisation time and reduce the costs associated with extensive experimental studies.

Ion-exchange chromatography is a well-established separation technique [3,4], utilising the variation in the electrostatic interaction between the stationary phase and the substances to achieve separation. Model-based optimisation of batch-wise separation using liquid chromatography has been applied to most kinds of chromatography processes, for example, hydrophobic interaction chromatography [5], reversed-phase chromatography [6] and ion-exchange chromatography [7]. The components involved in the above-mentioned processes are biomolecules, whereas in the case presented here the components are small ions, and elution is performed using a hot acid. Although the separation of europium by ion exchange using an acid is a known process [8,9], optimisation by means of modelling has not been widely studied. It is therefore of interest to investigate whether the models used, which were deigned to reproduce the separation of biomolecules, can describe the harsh environment in which a hot, strong acid is used to elute small metal ions.

The main objectives of this work were the calibration and validation of the model. The experimental system was then optimised using the model, with europium as the target component. A kinetic-dispersive column model was used to model the separation. Calibration was initiated by visual adjustment, after which

* Corresponding author. Tel.: +46 46 222 8088; fax: +46 46 222 4526.
E-mail address: bernt.nilsson@chemeng.lth.se (B. Nilsson).

0021-9673/$ – see front matter © 2011 Elsevier B.V. All rights reserved.
doi:10.1016/j.chroma.2011.11.028

computer simulations were used to achieve a better fit. The aim of process optimisation was to obtain a high-purity target component, at a reasonable production rate, while not wasting too much of the valuable metal, i.e. productivity and yield were used as object functions.

2. Theory

The model used in this work was a kinetic dispersive model [10] with a Langmuir mobile phase modulator (MPM) isotherm [11]. When using a kinetic dispersive model the resistance to mass transfer and the kinetics are lumped into one constant, here called $k_{kin,i}$ [10]. The Langmuir MPM model does not consider the interaction of the mobile phase with the stationary phase itself, but describes the modification of the mobile phase that causes the ions to bind to the stationary phase with varying degrees of strength.

2.1. Mobile phase

The concentration in the mobile phase, c, of each compound i changes with time according to the following relation [10]:

$$\frac{\partial c_i(z,t)}{\partial t} = D_{ax}\frac{\partial^2 c_i(z,t)}{\partial z^2} - v_{lin,i}\frac{\partial c_i(z,t)}{\partial z} + r_{ads,i} \quad (1)$$

where z is the axial coordinate along the column and D_{ax} describes the axial dispersion. The linear velocity, $v_{lin,i}$, is given by:

$$v_{lin,i} = \frac{F}{R_{col}^2\pi}\frac{1}{\varepsilon_c + (1-\varepsilon_c)\varepsilon_p K_{d,i}} \quad (2)$$

where F is the flow rate, R is the column radius, ε_c is the void in the column, ε_p is the porosity and $K_{d,i}$ is the exclusion factor. The adsorption term is calculated with the following relation.

$$r_{ads,i} = -\frac{1-\varepsilon_c}{\varepsilon_c + (1-\varepsilon_c)\varepsilon_p K_{d,i}}\frac{\partial q_i(z,t)}{\partial t} \quad (3)$$

2.2. Adsorption

According to the Langmuir MPM isotherm model, the concentration of one component on the surface of the stationary phase, q_i, changes as a function of time, t, according to [7]:

$$\frac{\partial q_i}{\partial t} = k_{ads,i}c_i q_{\max,i}\left(1 - \sum_{j=1}^{n_{comp}}\frac{q_j}{q_{\max,j}}\right) - k_{des,i}q_i \quad (4)$$

where n_{comp} the number of components modelled and $q_{\max,i}$ is the column capacity. The adsorption and desorption coefficients, $k_{ads,i}$ and $k_{des,i}$, can be described by

$$k_{ads,i} = k_{ads0,i}e^{\gamma_i s} \quad (5)$$

$$k_{des,i} = k_{des0,i}s^{\beta_i} \quad (6)$$

$k_{ads0,i}$ is a modulator constant, s is the concentration of the acid and the parameter β_i describes the ion-exchange characteristics. Since the model describes an ion-exchange process, the hydrophobicity, γ_i, was set to zero. The modulator constant $k_{des0,i}$ is a parameter describing the kinetics and is therefore denoted $k_{kin,i}$ in this work. The two modulator constants regarding the adsorbtion and desorption can be lumped into an equilibrium constant, $K_{eq,i}$:

$$K_{eq,i} = \frac{k_{ads0,i}}{k_{kin,i}} \quad (7)$$

Adding Eqs. (5) and (6) to Eq. (4) leads to this relation:

$$\frac{\partial q_i}{\partial t} = k_{kin,i}\left(c_i K_{eq,i} q_{\max,i}\left(1 - \sum_{j=1}^{n_{comp}}\frac{q_j}{q_{\max,j}}\right) - q_i s^{\beta_i}\right) \quad (8)$$

An initial estimate of $q_{\max,i}$ was obtained by using the following equation [6]:

$$q_{\max,i} = \frac{\Lambda}{\sigma_i + \nu_i} \quad (9)$$

where Λ is the total concentration of binding sites, σ_i is the number of sites blocked by the ion and ν the stoichiometric coefficient. The components considered here are small and assumed not to be subjected to steric hindrance, and thus σ_i was set to zero. The most stable oxidisation state of all the elements studied is +III [2], and it was therefore assumed that they all had the same ν, thus having the same $q_{\max}$. Assuming that the system is run in the linear range, the values of ν and β will be the same. $q_{\max}$ was defined as the number of moles of the bound component per m^3 gel, defining the gel as the particle including the pores. The porosity of the gel particles will therefore not influence this parameter.

3. Materials and methods

3.1. Materials

An Agilent 1200 series HPLC system with a 150 mm long, 4.6 mm diameter Eclipse XDB-C_{18} column was used throughout the experiments. The stationary phase was spherical silica gel with a bead diameter of 5 μm, modified with an ion-exchange ligand with a charge of −1. The ligand was chosen based on its ability to separate very similar metal ions, such as the rare-earth elements. The post-column reagent used to make the ions detectable under UV light was 0.1 g/l Arsenazo III, at a flow rate of 0.8 ml/min. UV absorbance was measured at 650 nm and 658 nm. In the eluent step, a gradient of nitric acid was used at a constant temperature of 60 °C and the flow rate of 1 ml/min. The experiments had a load step and an elution step. The elution started at an acid concentration of 7 mM and was run for 20 min.

The first data set consisted of overloaded gradient runs which were performed with different load volumes. Cerium was used for these experiments due to its similarity to the other elements, but lower cost. In the second data set, gradient experiments were run, having lower load volumes and a higher column ligand concentration. Three different gradient elution slopes were used in these

Table 1
The operating conditions used in the calibration and validation experiments.

	Column ligand concentration	Substances	Sample concentration	Load volume	Final buffer concentration
1st data set	2 wt%	Ce	10 mg/ml	100 μl 200 μl 400 μl	20 mM
2nd data set	5 wt%	Nd, Sm, Eu, Gd	500 ppm each	50 μl	250 mM 500 mM 1000 mM
Validation experiment	5 wt%	Nd, Sm, Eu, Gd	500 ppm each	50 μl	750 mM

experiments. These experiments were run using Nd, Sm, Eu and Gd. The experimental setup can be seen in Table 1.

3.2. Simulation

Throughout this work, the Preparative Chromatography Simulator, a tool developed at Lund University for the simulation of chromatographic separation, was used [12]. The finite-volume method was used in the simulations. The first-order derivative was described as a two-point backward difference, while the second-order derivative was described as a three-point central difference. The inlet boundary condition was a Robin condition, while the outlet condition was a homogeneous von Neumann condition. 1000 grid points were used. When solving differential equations, the solver *ode15s* in MATLAB was used, capable of solving stiff problems with fairly good accuracy.

3.3. Calibration

In order to achieve satisfactory optimisation, the objective of the calibration of the model was to define the correct positions of the peaks. This is mainly determined by $q_{\max}$, β and $K_{eq,i}$. $q_{\max}$ was calibrated by fitting the model to the results from the overloaded experiments. The gradient runs were not used for this purpose as the small load and concentration puts them in the linear region of the isotherm, thus making $q_{\max}$ difficult to decide. The experiments having varying gradient slopes were used to determine $K_{eq,i}$ and β. Visual calibration was carried out before the mathematical calibration. The visual calibration was used to determine the value of $k_{kin,i}$ and to identify good initial values for all parameters except β and $q_{\max}$. β was estimated to be around 3 based on the ionic charge on the ions and the ligand. The initial value of $q_{\max}$ was calculated using Eq. (9) and the known ligand density. The capacity of the column with the higher ligand concentration was scaled by the ligand density. Mathematical calibration of the model was performed with the function *fminsearch* in MATLAB, using the Nelder–Mead simplex algorithm. The absorbance measurements were recalibrated for each experiment due to interference with the reagent and eluting acid. ε_c was assumed to be 0.4, ε_p was estimated to be 0.6 and K_d was set to 1 for all components because of their small size.

After the initial visual calibration, automatic minimisation was carried out using *fminsearch*. The variables calibrated were $q_{\max}$ using the first data set, and $K_{eq,i}$, and β using the second data set. The objective function is given in Eq. (10).

$$res = \sum_{i=1}^{n_{\exp}} \left(\frac{\sum_{j=1}^{n_{\text{points}}} |c_{\exp,j} - c_{sim,j}|^2}{\sum_{k=1}^{n_{\text{points}}} |c_{\exp,k}|^2} \right)_i \tag{10}$$

Here c_{sim} is the simulated concentration in the mobile phase at the outlet, and $c_{\exp}$ is the experimentally determined concentration. Residuals were scaled by the peak concentration.

3.4. Optimisation

The target component for optimisation was europium as this is the most valuable of the elements studied. In order to run the process at an economically viable operating point, while taking into account both technical and economic aspects of chromatographic separation, optimisation was performed. The two objective functions used in the optimisation were productivity and yield, as both of these affect the production cost. The loading factor and the initial and final buffer strengths were optimised with respect to yield and productivity under a purity constraint of 99%. Optimisation was performed for a pre-selected number of decision variables, with lower and upper bounds, see Table 2.

Table 2
Decision variables used in the optimisation.

Decision variable	Lower boundary	Upper boundary
Load (column volumes)	0.01	6
Elution concentration (mol/m^3)		
Initial	50	150
Final	1000	20,000

The yield and the productivity are competing objectives, and therefore a population-based global optimiser, called differential evolution [13–15] was used. Optimising both objectives at once results in a Pareto front of the two competing objectives. The objective function for the productivity is defined as follows:

$$Pr_i = \frac{\int_{t_{cut1,i}}^{t_{cut2,i}} Fc_{out,i}\ dt}{t_{cycle} V_{col}} \tag{11}$$

where $t_{cutj,i}$ are the cut points of component i, F is the flow rate, $c_{out,i}$ is the outlet concentration of component i, t_{cycle} is the total cycle time, and V_{col} is the column volume. The yield objective function is defined as:

$$Y_i = \frac{\int_{t_{cut1,i}}^{t_{cut2,i}} Fc_{out,i}\ dt}{\int_{t_0}^{t_{load}} Fc_{feed,i}\, dt} \tag{12}$$

where t_0 and t_{load} are the times at which loading starts and stops.

4. Results and discussion

4.1. Calibration of the model

The initial estimate of the value of $q_{\max}$ was made by setting Λ to be 330 mol/m^3 in the 2 wt% column and assuming values of β and σ. The value of $k_{kin,i}$ was set to 3×10^{-3} (m^3/mol)$^\beta$/s for all the components as this gave a close fit to the experiments, while limiting the simulation time.

The overloaded experiments were used to determine $q_{\max}$. Due to saturation the overloaded peaks were cut off making the value of $q_{\max}$ difficult to calibrate. The calibration was therefore performed using the front and tails of the peaks, see Fig. 1. As $q_{\max}$ is correlated to other parameters such as $K_{eq,i}$ and β, a value of $q_{\max}$ that is the correct order of magnitude ensures that the model is sufficient for the purpose of this study. When studying the calibration using the gradient runs, the resulting close fit lead to the conclusion that this

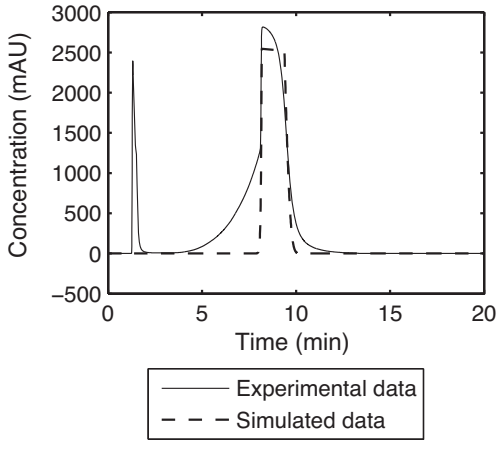

Fig. 1. Calibration to the overloaded data: (—) experimental data; (– –) simulated data. It was difficult to verify the fit to the experimental data as the experimental peaks were cut off, due to the detector being saturated. The fit of the curve was therefore only based on the points on the front and the back of the curve.

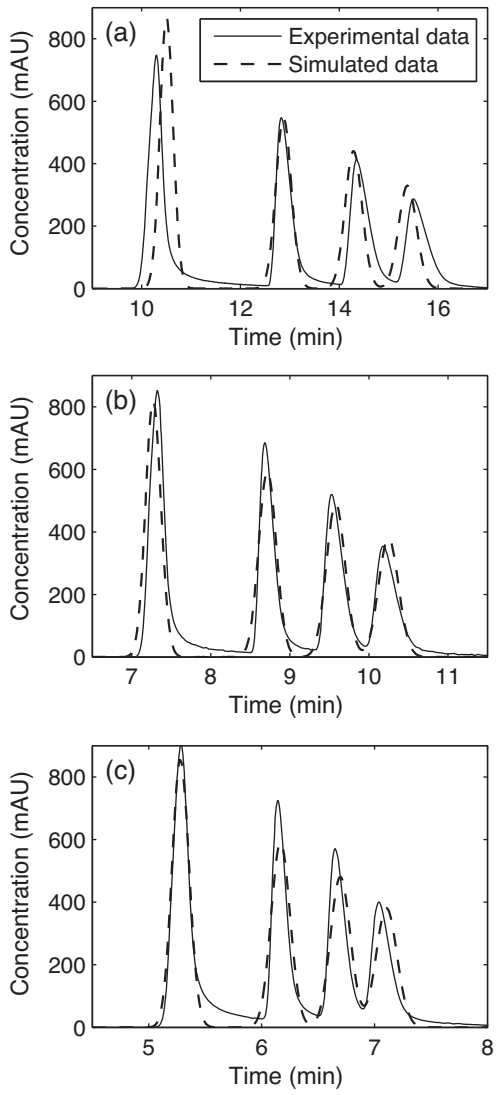

Fig. 2. Result from calibration using the second data set: (—) experimental data; (– –) simulated data. The gradient was run from an acid concentration of 7 mM to (a) 250 mM, (b) 500 mM and (c) 1000 mM. Sufficient agreement was obtained between the model and the experimental data. The elements were eluted in the order Nd, Sm, Eu and Gd, due to the higher ionic strength of atoms with higher atomic number.

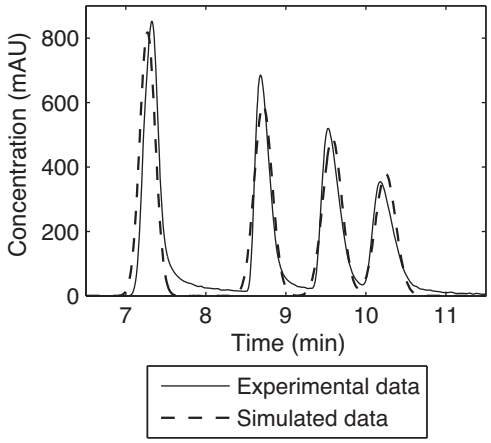

Fig. 3. Validation of the model: (—) experimental data; (– –) simulated data. A comparison between the calibrated model and an experiment executed with a slightly different gradient slope than used in the calibration experiments was evaluated. The model is considered to reproduce the real process sufficiently well for this study.

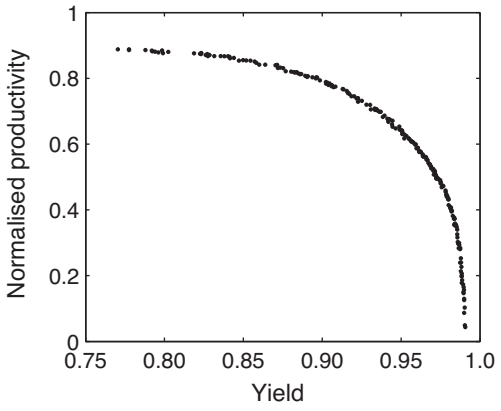

Fig. 4. The result of the mathematical optimisation. As the optimisation was conducted using the competing objectives' productivity and yield, the result was a Pareto front showing the relation between these two.

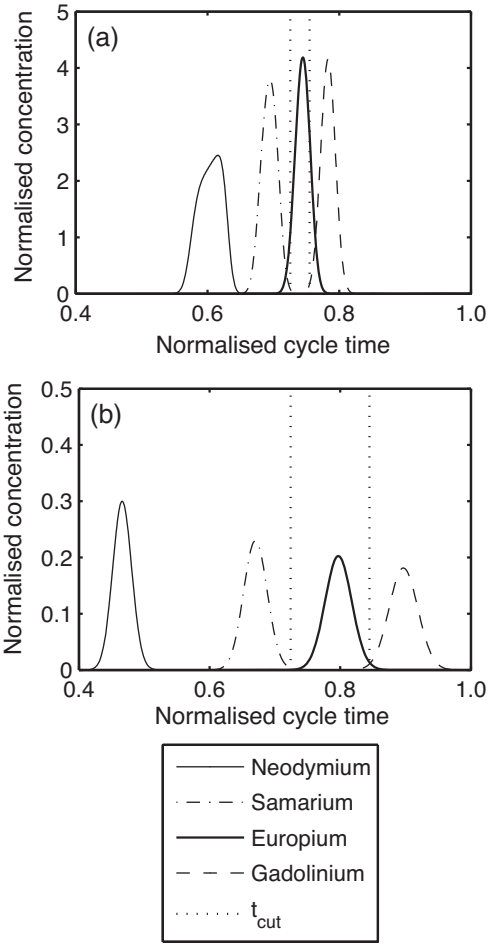

Fig. 5. The chromatograms corresponding to the two extreme points on the Pareto front having (a) maximum productivity and (b) maximum yield: (—) Nd; (–·–) Sm; (**—**) Eu; (– –) Gd; (· · ·) t_{cut}. Note the difference in the order of magnitude on the y-axis in the two figures.

was achieved, see Fig. 2. The values resulting from calibration are listed in Table 3.

The validation of the model was a comparison with an experiment having a slightly different gradient slope than the experiments used for calibration. The result can be seen in Fig. 3. This proved that the model fits the experimental data adequately well for the purpose of this work.

Table 3
The calibrated model parameter values.

Parameter	Value
q_{max} (mol/m^3 gel) 5 wt% column	700
β	2.3
$K_{eq} \times 10^{-4}$ ((mol/m^3)$^{\beta-1}$)	
Neodymium	130
Samarium	280
Europium	400
Gadolinium	530

4.2. Optimisation

The separation process was optimised for europium. The Pareto front in Fig. 4 shows the trade-off between the productivity and the yield. With the parameter bounds used, a yield of 100% could not be attained, as a result of too high load.

The choice of the point on the Pareto front to use is dependent on the use and constraints of the system. One way choosing is by multiplying the productivity and yield for each point, choosing the maximum value achieved [16]. The corresponding chromatograms to the two extreme points of the Pareto front can be seen in Fig. 5. When maximising the productivity the result is a shorter cycle time, while maximising the yield results in separation closer to baseline separation.

5. Conclusions

The model commonly used to depict separation of larger molecules was able to reproduce the separation of the rare-earth elements adequately. Cerium was found to be a suitable substitute for the more expensive elements Nd, Sm, Eu and Gd when performing overloaded experiments. Optimisation of the separation of europium, regarding productivity and yield, resulted in a Pareto front. The study has shown that it is possible to both model and optimise the harsh system used to separate small ions in a hot strong acid.

Nomenclature

c_i	mobile phase concentration of component i (mol/m^3)
c_{exp}	experimentally determined mobile phase concentration (mol/m^3)
$c_{feed,i}$	concentration of component i in the feed (mol/m^3)
$c_{out,i}$	concentration of component i at the outlet (mol/m^3)
c_{sim}	simulated concentration (mol/m^3)
D_{ax}	axial dispersion (m^2/s)
F	flow rate (m^3/s)
$k_{ads,i}$	adsorption coefficient (m^3/mol/s)
$k_{ads0,i}$	modulator constant (m^3/mol/s)
$K_{d,i}$	exclusion factor for component i
$k_{des,i}$	desorption coefficient (s^{-1})
$k_{des0,i}$	kinetic constant for component i ((m^3/mol)$^\beta$/s)
$K_{eq,i}$	equilibrium constant of component i ((mol/m^3)$^{\beta-1}$)
$k_{kin,i}$	kinetic constant for component i ((m^3/mol)$^\beta$/s)
Pr_i	productivity (kg/(s·m^3 stationary phase))
q_i	concentration of component i on the surface of the stationary phase (mol/m^3 gel)
$q_{max,i}$	the column capacity for component i (mol/m^3 gel)
R_{col}	column radius (m)
$r_{ads,i}$	adsorption term of component i (mol/m^3/s)
res	residual
s	acid concentration (mol/m^3)
t	time (s)
t_0	the time at which loading starts (s)
$t_{cut1,i}$	time of first cut point (s)
$t_{cut2,i}$	time of second cut point (s)
t_{cycle}	total cycle time (s)
t_{load}	the time at which loading stops (s)
V_{col}	volume of the column (m^3)
$v_{lin,i}$	linear velocity (m/s)
Y_i	yield of component i
z	axial coordinate along the column (m)
β_i	parameter describing the ion-exchange characteristics
γ_i	hydrophobicity constant (m^3/mol)
ε_c	void in the column
ε_p	porosity of the particles
Λ	total concentration of binding sites (mol/m^3 gel)
ν_i	stoichiometric coefficient of component i
σ_i	number of binding sites blocked by component i

Acknowledgement

The authors would like to take the opportunity to thank Stiftelsen för Strategisk Forskning for their support in this work.

References

[1] J.B. Hedrick, 2006 Minerals Yearbook – Rare Earths, U.S. Geological Survey, 2006.
[2] I. McGill, Ullmann's Encyclopedia of Industrial Chemistry, Wiley-VCH, 2005.
[3] G. Carta, A. Jungbauer, Protein Chromatography: Process Development and Scale-Up, Wiley-VCH, Weinheim, 2010.
[4] A.A. Zagorodni, Ion Exchange Materials, Elsevier, Oxford, 2007.
[5] N. Jacobsson, M. Degerman, B. Nilsson, J. Chromatogr. A 1099 (2005) 157.
[6] M. Degerman, N. Jacobsson, B. Nilsson, J. Chromatogr. A 1162 (2007) 41.
[7] D. Karlsson, N. Jacobsson, A. Axelsson, B. Nilsson, J. Chromatogr. A 1055 (2004) 29.
[8] J.G. Crock, F.E. Lichte, G.O. Riddle, C.L. Beech, Talanta 33 (1986) 601.
[9] Y. Inoue, H. Kumagai, Y. Shimomura, T. Yokoyama, T.M. Suzuki, Anal. Chem. 68 (1996) 1517.
[10] H. Schmidt-Traub, Preparative Chromatography of Fine Chemicals and Pharmaceutical Agents, Wiley-VCH, Weinheim, 2005.
[11] W.R. Melander, Z. El Rassi, C. Horváth, J. Chromatogr. A 469 (1989) 3.
[12] http://www.chemeng.lth.se/pcs, Department of Chemical Engineering, Lund, 2011.
[13] K. Price, R.M. Storn, J.A. Lampinen, A Practical Approach to Global Optimization, Springer-Verlag, Berlin, 2005.
[14] J. Lampinen, Proceedings of the 2002 Congress on Evolutionary Computation, Honolulu, HI, USA, 2002, p. 1468.
[15] J.A. Adeyemo, F.A.O. Otieno, J. Appl. Sci. 9 (2009) 3652.
[16] A. Felinger, G. Guiochon, J. Chromatogr. A 752 (1996) 31.